

单层镍锰层状双金属氢氧化物用于锂-氧电池双功能催化剂

侯雪丹¹ 郭守武^{*,1} 王 倩² 王晓飞^{*,1}

(¹ 陕西科技大学材料科学与工程学院, 西安 710021)

(² 西安工业大学材料与化工学院, 西安 710021)

摘要: 将块体镍锰层状双金属氢氧化物(Ni₃Mn-LDHs)通过液相剥离法制备成单层 Ni₃Mn-LDHs,然后采用自组装法获得 Ni₃Mn-LDHs/CNT 复合材料。采用 X 射线衍射(XRD)、扫描电镜(SEM)、透射电镜(TEM)对复合材料的结构进行分析,通过恒流充放电、循环伏安(CV)和电化学阻抗谱(EIS)研究电极的电化学过程。结果表明,Ni₃Mn-LDHs/CNT 复合材料可以有效提升 ORR 和 OER 的催化活性,与 CNT 正极相比较,Ni₃Mn-LDHs/CNT 正极在锂-氧电池中的放电容量提高了近 300%,并且具有优异的倍率性能和循环稳定性。

关键词: 复合材料; 锂-氧电池; 催化剂; 功能性

中图分类号: O614.71+1; O614.81+3

文献标识码: A

文章编号: 1001-4861(2018)10-1910-07

DOI: 10.11862/CJIC.2018.237

Single-Layer Ni₃Mn-Layered Double Hydroxides as Bifunctional Catalyst for Rechargeable Li-O₂ Batteries

HOU Xue-Dan¹ GUO Shou-Wu^{*,1,2} WANG Qian³ WANG Xiao-Fei^{*,1}

(¹*School of Materials Science and Engineering, Shaanxi University of Science and Technology, Xi'an 710021, China*)

(²*School of Materials Science and Chemical Engineering, Xi'an Technological University, Xi'an 710021, China*)

Abstract: Bulk Ni₃Mn-layered double hydroxides (Ni₃Mn-LDHs) was exfoliated into single-layer Ni₃Mn-LDHs nanosheets via liquid phase exfoliation, and then incorporated with CNT to obtain Ni₃Mn-LDHs/CNT composites by self-assemble method. The structure of the composites was characterized by X-ray powder diffraction (XRD), scanning electron microscopy (SEM) and transmission electron microscopy (TEM). The electrochemical process was analyzed by galvanostatic tests, cyclic voltammetry (CV) and electrochemical impedance spectroscopy (EIS). The Ni₃Mn-LDHs/CNT composites improved the ORR and OER catalytic activities significantly, the obtained Ni₃Mn-LDHs/CNT cathode presented nearly 300% higher discharge capacity, excellent rate and cycling stability than the CNT cathode in lithium-oxygen batteries.

Keywords: composite materials; lithium-oxygen batteries; catalyst; functional

0 Introduction

Lithium-oxygen (Li-O₂) batteries have captured significant scientific interest due to their ultrahigh

theoretical energy density of ~3 505 Wh·kg⁻¹ [1-5]. However, the current Li-O₂ batteries suffer from sluggish kinetics of oxygen reduction reaction (ORR) and oxygen evolution reaction (OER) during the

收稿日期: 2018-05-15。收修改稿日期: 2018-08-17。

国家自然科学基金(No.51608412)、陕西省自然科学基金(No.2016JQ2034)、陕西省教育厅专项基金(No.17JK0086)和陕西科技大学科研启动基金(No.2016BJ-48)资助项目。

*通信联系人。E-mail: swguo@sjtu.edu.cn, wangxiaof@sust.edu.cn, Tel: 029-86168688

discharge/charge processes. Developing low cost and high-efficient air cathode is one of the effective methods to improve the electrochemical performance of Li-O₂ batteries^[6-9].

In the majority of cases, carbon material such as carbon nanotube (CNT), reduced graphene oxide and carbon aerogels have been widely employed as cathode for Li-O₂ battery due to their high conductivity, light weight, especially for CNT, which possess unique features such as high aspect ratio, low cost and abundant pore structure^[10]. Although CNT-based air cathode have been proved to be feasible cathode for Li-O₂ battery, bare CNT usually suffers from high overpotential and low capacity due to the low ability in promoting the formation/decomposition of ideal discharge product-Li₂O₂, as a remedy, combining or depositing high-efficient electrocatalysts with excellent ORR and OER activity on CNT is one of the efficiency way to increase the overall cathode activity^[11]. So far, various catalysts such as noble metals, transition metal oxides and perovskite oxides have been widely studied as ORR or OER catalysts^[12-17]. Although noble metals exhibit superior catalytic properties, the high cost and element scarcity limit their widespread application. Layered double hydroxides (LDHs), a class of multi-metal hydrotalcite-like compounds, have recently attracted extensive interest due to their considerable catalytic activities even superior to that of noble metals, the general formula of LDHs is $[M^{2+}_{1-x}M^{3+}_x(OH)_2]^{x+}[A^{n-}]_{x/n} \cdot yH_2O$, where M^{2+} , M^{3+} and A^{n-} represent the divalent, trivalent metal cations and charge compensating anions^[18], because of the unique characteristics such as composition flexibility, ease of preparation, high redox activity and low cost, making LDHs as an ideal alternative to precious metals in Li-O₂ batteries^[19-21]. The unique properties mainly derives its metal-contained layered matrix, and especially transition metal cations contained LDH materials, such as Ni, Co, Fe and Mn-containing LDHs, have exhibited excellent electrocatalytic activity, especially for OER^[22]. Unfortunately, the poor electronic conductivity and large particle size of the bulk LDHs are the major problems to be overcome. Liquid phase

exfoliation is a facile method to enhance the catalytic activity of bulk LDHs. The exfoliated single-layer nanosheets have the same chemical compositions but significantly higher OER activity, more exposed active sites and faster charge transfer compared to the bulk LDHs, and the exfoliated thin single-layer nanosheets also facilitate the improvement of the electronic conductivity^[23-25], but the catalytic performance of the exfoliated single-layer LDHs has not been revealed in Li-O₂ batteries up to now.

Herein, Ni₃Mn-LDHs was prepared and exfoliated into single-layered LDHs by a facile liquid phase exfoliation, then incorporated with CNT via self-assemble method, the as-prepared Ni₃Mn-LDHs/CNT composites demonstrated excellent electrochemical performance in Li-O₂ batteries.

1 Experimental

1.1 Materials synthesis

Typically, NiCl₂·6H₂O (1.426 2 g), MnCl₂·4H₂O (0.395 8 g), and Hexamethylenetetramine (HMT, 0.7 g) were dissolved in 60 mL deionized water and heated at 100 °C for 12 h to form bulk Ni₃Mn-LDHs. Then, 0.1 g bulk Ni₃Mn-LDHs were introduced into 50 mL formamide solution, magnetic stirring for 24 h and centrifuged under 1 500 r·min⁻¹ for 30 min to obtain single-layer Ni₃Mn-LDHs colloidal suspension (positively charged LDHs). Negatively charged CNT was obtained by treating CNT in H₂SO₄/HNO₃ solution ($V_{H_2SO_4}/V_{HNO_3}=3$). The Ni₃Mn-LDHs/CNT sample was obtained through the following electrostatic self-assembly. 50 mL single-layer Ni₃Mn-LDHs colloidal suspension (1.2 mg·mL⁻¹) was added dropwise into 50 mL acidification CNT (1 mg·mL⁻¹) under magnetic stirring over the course of 1 h. The the resulting suspension was then standing at room temperature for 24 h. The final product was isolated by centrifugation, washed with copious amounts of deionized water until the pH value is about 7, and were placed in a vacuum oven and dried at 80 °C for 24 h.

1.2 Characterization and electrochemical measurement

The samples were characterized by X-ray

diffraction (XRD, Rigaku D/Max2200 V/PC), with Cu $K\alpha$ radiation ($\lambda=0.154\ 06\ \text{nm}$) at a scan speed of $8^\circ \cdot \text{min}^{-1}$. The operating voltage was 40 kV and the current was 40 mA. The operating voltage of scanning electron microscopy (SEM, JEOL S4800) was 5 kV and transmission electron microscopy (TEM, FEI Tecnai G2 F20 S-TWIN). Swagelok-type Li-O₂ batteries containing a Li foil anode, a nickel foam cathode, a celgard 2500 membrane and 100 μL electrolyte (0.9 mol $\cdot \text{L}^{-1}$ lithium bis(trifluoromethanesulfonyl)imide (LiTFSI) in tetraethylene glycol dimethyl ether (TEGDME)) was assembled inside an Ar-filled glove box. The air cathodes were prepared by mixing 90% (*w/w*) CNT or Ni₃Mn-LDHs/CNT and 10% (*w/w*) polyvinylidene fluoride (PVDF) in a mortar. A few drops of *N*-methyl pyrrolidone (NMP) was added and ultrasound to form an ink. The ink was pasted onto nickel foam current collector ($1.5\ \text{cm}^2$). Comparable air cathode (Ni₃Mn-LDHs + CNT cathode) was also fabricated by coating a mixture of Ni₃Mn-LDHs, CNT and PVDF in a conventional weight ratio of 3:6:1 on the nickel foam current collector ($1.5\ \text{cm}^2$). These cathodes were dried at 110 $^\circ\text{C}$ under vacuum for 12 h. After standing 2 h, The galvanostatic tests were

carried out using a Neware battery testing system with a potential range of 2.0~4.5 V. The capacities and current densities were calculated based on the mass of CNT (for the CNT and Ni₃Mn-LDHs+CNT cathodes) or Ni₃Mn-LDHs/CNT (for the Ni₃Mn-LDHs/CNT cathode). The electrochemical impedance spectroscopy (EIS) was recorded using CHI660E electrochemical workstation in the frequency range from 100 kHz to 10 mHz. Cyclic voltammetry (CV) was also recorded using CHI660E electrochemical workstation at a scan rate of $0.5\ \text{mV} \cdot \text{s}^{-1}$.

2 Results and discussion

Fig.1(a) shows the XRD patterns of the CNT, bulk Ni₃Mn-LDHs and Ni₃Mn-LDHs/CNT composites. The peaks at 2θ values of 11.34° , 34.41° and 59.98° corresponded to the (003), (012) and (110) crystal planes of Ni₃Mn-LDHs, respectively^[26]. The peak at 26.5° and 43.5° indicated the present of CNT in the Ni₃Mn-LDHs/CNT composites, however, only one significant diffraction peak at 11.34° was in accordance with the peaks of the bulk Ni₃Mn-LDHs, maybe the exfoliated single-layer Ni₃Mn-LDHs decreased the crystallinity of Ni₃Mn-LDHs. From the SEM image in

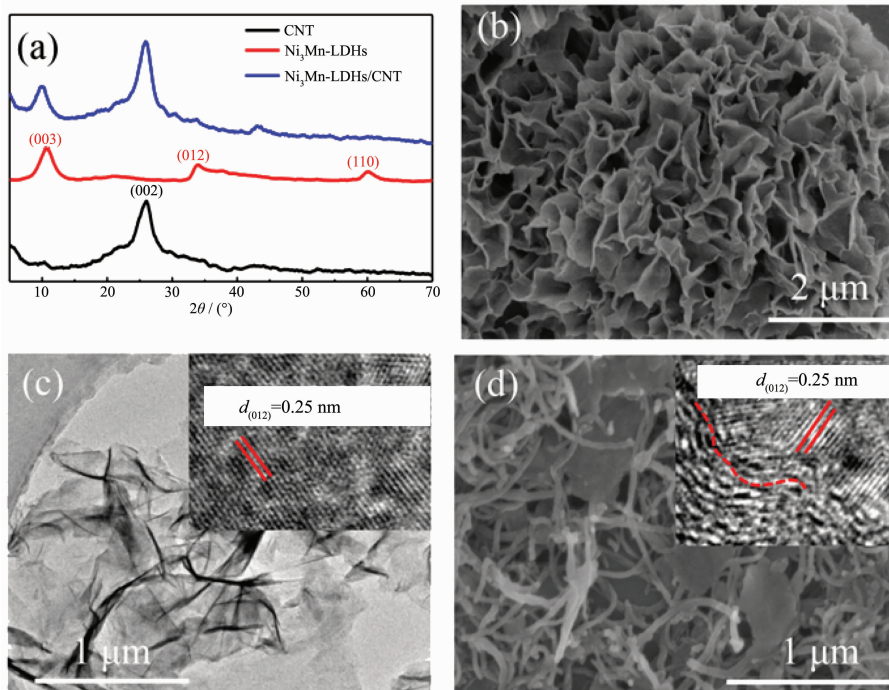


Fig.1 (a) XRD patterns of CNT, Ni₃Mn-LDHs and Ni₃Mn-LDHs/CNT; (b) SEM image of bulk Ni₃Mn-LDHs; (c) TEM image of single-layer Ni₃Mn-LDHs nanosheets; (d) SEM image of Ni₃Mn-LDHs/CNT

Fig.1(b) it could be found that the bulk $\text{Ni}_3\text{Mn-LDHs}$ nanosheets presented a flower-like structure, and the average diameter size was about $2.35\ \mu\text{m}$ and thickness was approximate $10\ \text{nm}$. However, only single nanosheets with an average lateral size of about $400\ \text{nm}$ could be found after exfoliation, indicating that the exfoliation process destroyed its original structure, the HRTEM image insert in Fig.1(c) presents that the interplanar spacing is $0.25\ \text{nm}$, corresponding to the (012) plane of $\text{Ni}_3\text{Mn-LDHs}$, as shown in Fig.1(c), indicating the delaminated small scale single-layer nanosheets maintained the unique structure of bulk $\text{Ni}_3\text{Mn-LDHs}$. Fig.1(d) shows the SEM image of the obtained composites, it could be found that the single-layer $\text{Ni}_3\text{Mn-LDHs}$ mixed uniformly with CNT, which ensure the maximum contact of $\text{Ni}_3\text{Mn-LDHs}$ with CNT and lead to a fast electron transport during the discharge-charge processes, from the HRTEM image insert in Fig.1(d) it could be found that there were slightly lattice distortions at the interfaces, facilitating to create more active sites and promote the catalytic performance^[27-28].

Fig.2(a) shows the first discharge-charge curves of Li- O_2 batteries with CNT, $\text{Ni}_3\text{Mn-LDHs}+\text{CNT}$ and

$\text{Ni}_3\text{Mn-LDHs/CNT}$ cathode cathodes at $100\ \text{mA}\cdot\text{g}^{-1}$, the discharge capacities of the CNT, $\text{Ni}_3\text{Mn-LDHs}+\text{CNT}$ and $\text{Ni}_3\text{Mn-LDHs/CNT}$ cathode were $1\ 449$, $1\ 845$ and $3\ 476\ \text{mAh}\cdot\text{g}^{-1}$, respectively, the higher discharge capacity of the $\text{Ni}_3\text{Mn-LDHs/CNT}$ and $\text{Ni}_3\text{Mn-LDHs}+\text{CNT}$ electrodes than the bare CNT electrode indicated that the introduction of $\text{Ni}_3\text{Mn-LDHs}$ catalyst into air cathode could enhanced the discharge capacity, enhancing the ORR process. More importantly, compared with the $\text{Ni}_3\text{Mn-LDHs}+\text{CNT}$ electrode, it was interesting to find that the discharge-charge voltage gap of the $\text{Ni}_3\text{Mn-LDHs/CNT}$ electrode was significantly lower and delivered higher discharge capacity, this probably due to the maximum contact of $\text{Ni}_3\text{Mn-LDHs}$ with CNT. Meanwhile, the results also indicated that the exfoliated $\text{Ni}_3\text{Mn-LDHs}$ enhanced OER/ORR catalytic activity although they have the same chemical structure as the bulk LDHs, and the increased defects that derived from the lattice distortion provided more active sites and facilitating the deposition of the discharge products.

Further information could be achieved from EIS tests at open circuit voltage (OCV), as shown in Fig.2 (b), although the three cathodes have the same

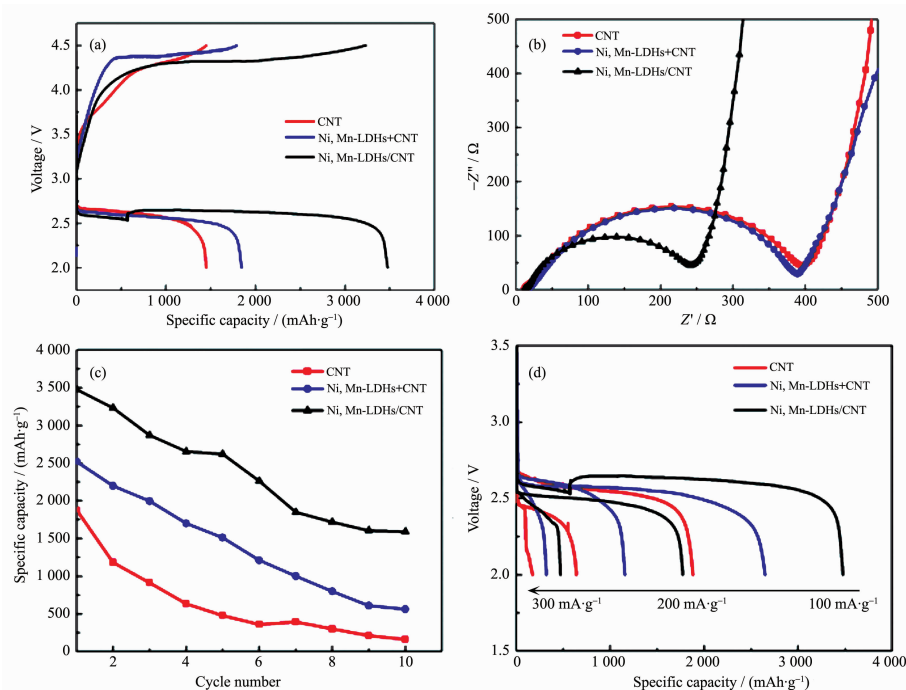


Fig.2 (a) First discharge-charge curves, (b) EIS spectra at OCV, (c) cycle ability and (d) rate performance of the CNT, $\text{Ni}_3\text{Mn-LDHs}+\text{CNT}$ and $\text{Ni}_3\text{Mn-LDHs/CNT}$ electrodes

interfacial electron transfer in the high-frequency region, which is related to the contact between the air cathode and the electrolyte, the charge transfer resistance (R_{ct}) which is related to the charge transfer reaction were obviously different, the $\text{Ni}_3\text{Mn-LDHs/CNT}$ cathode exhibited lowest R_{ct} than that of the $\text{Ni}_3\text{Mn-LDHs+CNT}$ and CNT electrodes, indicating the fastest kinetics of ORR^[29]. In other words, the high catalytic active of the $\text{Ni}_3\text{Mn-LDHs/CNT}$ cathode facilitated the nucleation of Li_2O_2 ^[30-31]. Based on above results, we further compared the rate and cycling performance with the bare CNT to reveal the excellent OER/ORR activities of $\text{Ni}_3\text{Mn-LDHs/CNT}$ cathode. Fig.2(c,d) shows the corresponding full discharge-charge cycling stability at $100\text{ mA}\cdot\text{g}^{-1}$ and rate performance, respectively, the 10th discharge capacity of the $\text{Ni}_3\text{Mn-LDHs/CNT}$ cathode decayed to 45.7%, the $\text{Ni}_3\text{Mn-LDHs+CNT}$ cathode decayed to 22.4% and the CNT cathode decay to 8.5% of the first discharge capacity. Although the specific capacity decreased upon increasing the current density for all cathodes, the capacity of the $\text{Ni}_3\text{Mn-LDHs/CNT}$ cathode was higher than that of the $\text{Ni}_3\text{Mn-LDHs+CNT}$ cathode and the CNT cathode, the capacity retentions of the

$\text{Ni}_3\text{Mn-LDHs/CNT}$ cathode at 200 and $300\text{ mA}\cdot\text{g}^{-1}$ were 51.1% and 13.3%, respectively, while the corresponding $\text{Ni}_3\text{Mn-LDHs+CNT}$ cathode exhibited low capacity retentions of about 43.6% and 27.7%, respectively, and CNT cathode only exhibited an low capacity retentions of about 34.1% and 9.1%, respectively, further conforming the enhanced reaction kinetics of the $\text{Ni}_3\text{Mn-LDHs/CNT}$ cathode.

The enhanced ORR catalysis of the $\text{Ni}_3\text{Mn-LDH}$ could be further confirmed from the CV curves, as shown in Fig.3(a), for the ORR process, it was clearly to find that the peak current of the $\text{Ni}_3\text{Mn-LDHs/CNT}$ cathode is much higher than that of the $\text{Ni}_3\text{Mn-LDHs+CNT}$ cathode and CNT cathode, meanwhile, only one cathodic peak is observed for all cathodes, suggesting the formation of one kind of discharge product (Li_2O_2) for all cathodes. And the $\text{Ni}_3\text{Mn-LDHs/CNT}$ cathode also exhibited slightly higher peak current during the following OER process, indicating the improved OER catalytic activity. From the SEM analysis in Fig.3(b~d), it could be found that all first discharged cathodes exhibited film-like Li_2O_2 , however, the first discharged of CNT cathode contained many large and compact particles while the first discharged of $\text{Ni}_3\text{Mn-LDHs/}$

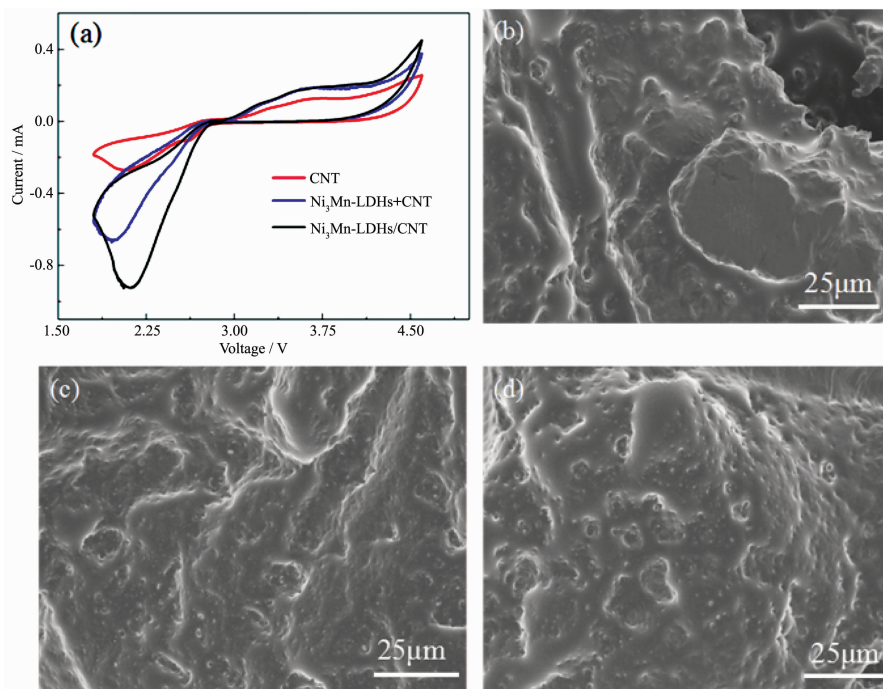


Fig.3 (a) CV curves of the CNT, $\text{Ni}_3\text{Mn-LDHs+CNT}$ and $\text{Ni}_3\text{Mn-LDHs/CNT}$ cathodes, SEM images of the first discharged of CNT (b), $\text{Ni}_3\text{Mn-LDHs+CNT}$ (c) and $\text{Ni}_3\text{Mn-LDHs/CNT}$ (d) electrodes

CNT and $\text{Ni}_3\text{Mn-LDHs}+\text{CNT}$ cathode revealed a relative smaller and looser surface than that of the discharged CNT cathode. Based on the high discharge capacity, the improved ORR/OER processes and the different SEM images of the $\text{Ni}_3\text{Mn-LDHs}/\text{CNT}$ cathode, we have reason to believe that the introduced $\text{Ni}_3\text{Mn-LDHs}/\text{CNT}$ caused the improvement of the electrochemical performance of the Li- O_2 battery.

Commonly, capacity-limiting cycle is another widely used test to evaluate the cyclability of a specific cathode material, and the cycling performances were conducted with a limited specific capacity of $500 \text{ mAh} \cdot \text{g}^{-1}$ at a current density of $100 \text{ mA} \cdot \text{g}^{-1}$. however, the CNT cathode and $\text{Ni}_3\text{Mn-LDHs}+\text{CNT}$ cathode rapidly

failed within 20 cycles even using the capacity-limiting cycling protocol, as shown in Fig.4(a~d), and the charge potential almost maintained the same with that of the full discharge/charge CNT cathode and $\text{Ni}_3\text{Mn-LDHs}+\text{CNT}$ cathode. When the $\text{Ni}_3\text{Mn-LDHs}/\text{CNT}$ cathode is cycled with a limited capacity output of $500 \text{ mAh} \cdot \text{g}^{-1}$, no capacity loss could be found over 30 cycles, and the 30th charge potential was even lower than that of the first charge potential of the CNT cathode, as shown in Fig.4(e~f), meanwhile, it is clear to find that the first charge potential dropped to 3.5 V, which was about 750 mV lower than the charge potential under full discharge/charge conditions, this phenomenon was also observed in our previous

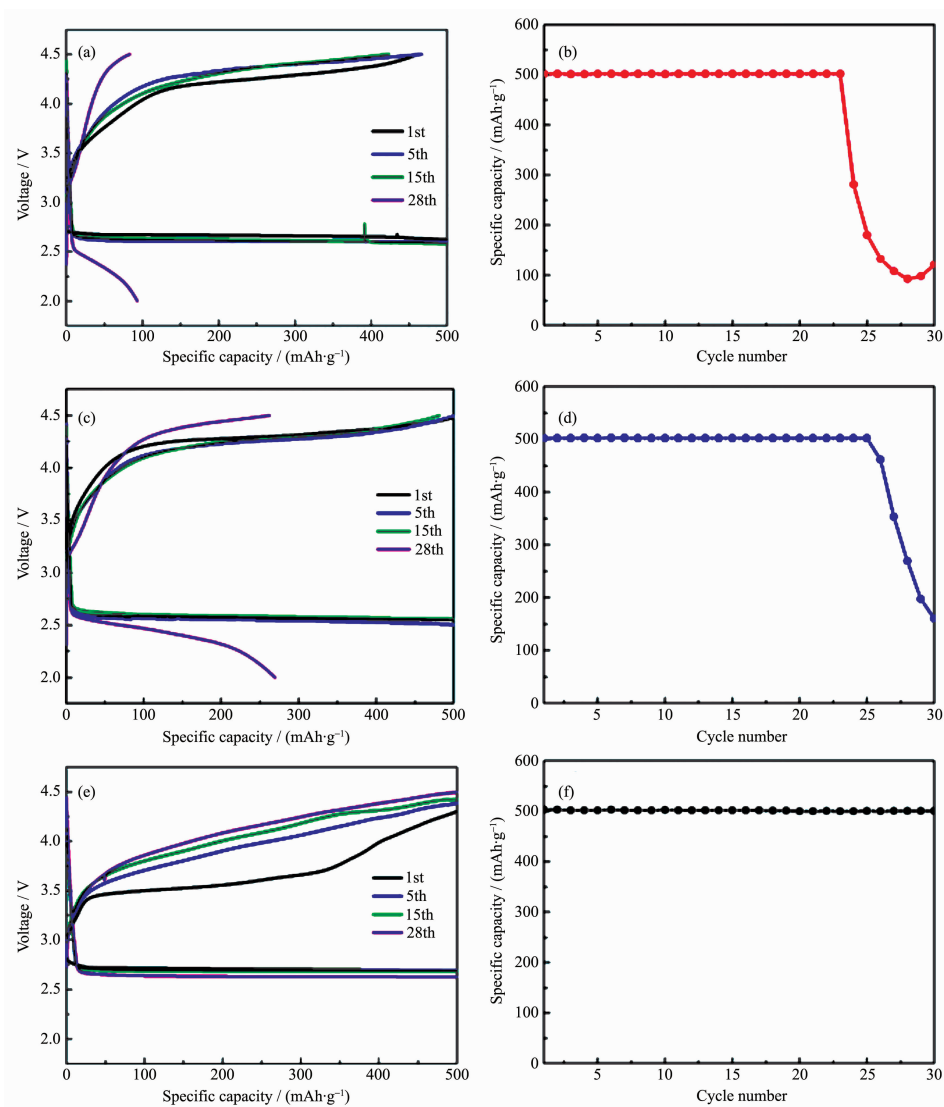


Fig.4 Discharge-charge curves and cycling performances of the (a, b) CNT, (c, d) $\text{Ni}_3\text{Mn-LDHs}+\text{CNT}$ and (e, f) $\text{Ni}_3\text{Mn-LDHs}/\text{CNT}$ electrodes

research because a slight amount of the discharge product could be easily decomposed^[32]. Based on the above results, it is speculated that excellent performance of Ni₃Mn-LDHs/CNT can be attributed to the following reasons: Firstly, the exfoliated single-layer Ni₃Mn-LDHs nanosheets exposed more active sites and enhance the catalytic activity; Secondly, the incorporation of Ni₃Mn-LDHs with CNT induced the generation of lattice distortions, the altered surface state of the composite facilitated the exposure of defects and enhanced the adsorption and dissociation of oxygen^[33]. In other words, the unique structure of Ni₃Mn-LDHs/CNT composites promoted the deposition and decomposition of the discharge products.

3 Conclusions

In this work, bulk Ni₃Mn-LDHs was exfoliated into single-layer nanosheets and then incorporated with CNT via a self-assemble method. The formed composites facilitated the ORR/OER kinetics of the cathode and thus significantly improve the discharge capacity, rate and cycling performances of the Li-O₂ batteries. The facile and synthetic strategy can be easily extended to other LDHs-based composites.

References:

- [1] Bruce P G, Freunberger S A, Hardwick L J, et al. *Nat. Mater.*, **2012**,**11**:19-29
- [2] CAI Sheng-Rong(蔡生荣), WANG Xiao-Fei(王晓飞), ZHU Ding(朱丁), et al. *Chinese J. Inorg. Chem.*(无机化学学报), **2016**,**32**(12):2082-2087
- [3] Wang J, Yin Y B, Liu T, et al. *Nano Res.*, **2018**,**11**:3434-3441
- [4] Liu Q C, Chang Z W, Li Z J, et al. *Small Methods*, **2018**,**2**: 1700231(16 Pages)
- [5] Xu J J, Zhang X B. *Nat. Energy*, **2017**,**2**:1-2
- [6] Chang Z, Xu J J, Zhang X B. *Adv. Energy Mater.*, **2017**,**7**:1-21
- [7] Zhang P, Zhao Y, Zhang X B. *Chem. Soc. Rev.*, **2018**,**47**: 2921-3004
- [8] Yang Z D, Chang Z W, Zhang Q, et al. *Sci. Bull.*, **2018**,**63**: 433-440
- [9] Xu J J, Chang Z W, Yin Y B, et al. *ACS Cent. Sci.*, **2017**,**3**: 598-604
- [10] Zhu Q C, Du F H, Xu S M, et al. *ACS Appl. Mater. Interfaces*, **2015**,**8**:3868-3873
- [11] Yang X Y, Xu J J, Chang Z W, et al. *Adv. Energy Mater.*, **2018**,**8**:1-7
- [12] Jung J W, Choi D W, Lee C K, et al. *Nano Energy*, **2018**,**46**: 193-202
- [13] Kim J G, Kim Y, Noh Y, et al. *ACS Appl. Mater. Interfaces*, **2018**,**10**:5429-5439
- [14] Gao R, Yang Z, Zheng L, et al. *ACS Catal.*, **2018**,**8**:1955-1963
- [15] Chang Z W, Meng F L, Zhong H X, et al. *Chin. J. Chem.*, **2018**,**36**:287-292
- [16] Meng F L, Chang Z, Xu J, et al. *Mater. Horiz.*, **2018**,**5**:298-302
- [17] Yang Z D, Chang Z W, Xu J J, et al. *Sci. China Chem.*, **2017**,**60**:1540-1545
- [18] Wang Q, O'Hare D. *Chem. Rev.*, **2012**,**112**:4124-4155
- [19] Chitravathi S, Kumar S, Munichandraiah N. *RSC Adv.*, **2016**, **6**:103106-103115
- [20] Xu S M, Zhu Q C, Long J, et al. *Adv. Funct. Mater.*, **2016**, **26**:1365-1374
- [21] Liu Y, Liu Y, Shi H H, et al. *J. Alloys Compd.*, **2016**,**688**: 380-387
- [22] Shao M F, Zhang R K, Li Z H, et al. *Chem. Commun.*, **2015**,**51**:15880-15893
- [23] Song F, Hu X L. *Nat. Commun.*, **2014**,**5**:1-9
- [24] Zhao M M, Zhao Q X, Li B, et al. *Nanoscale*, **2017**,**9**:15206-15225
- [25] Liang J B, Ma R Z, Iyi N, et al. *Chem. Mater.*, **2010**,**22**:371-378
- [26] Jia G, Hu Y F, Qian Q F, et al. *ACS Appl. Mater. Interfaces*, **2016**,**8**:14527-14534
- [27] Sun Y F, Gao S, Lei F C, et al. *Chem. Soc. Rev.*, **2014**,**44** (3):623-636
- [28] Voiry D, Yamaguchi H, Li J W, et al. *Nat. Mater.*, **2013**,**12** (9):850-855
- [29] Duan X, Song M, Zhang L, et al. *New J. Chem.*, **2017**,**41**: 12789-12794
- [30] Zhu X, Yan Y, Wan W, et al. *Mater. Lett.*, **2018**,**215**:71-74
- [31] YI Luo-Cai(易罗财), CI Su-Qin(次素琴), SUN Cheng-Li(孙成丽), et al. *Prog. Chem.*(化学进展), **2016**,**28**(8):1251-1264
- [32] Wang X F, Wang Q, Hou X D, et al. *J. Alloys Compd.*, **2018**,**744**:196-203
- [33] Wang F, Li H, Wu Q, et al. *Electrochim. Acta*, **2016**,**202**:1-7